This article has been accepted for publication in a future issue of this journal, but has not been fully edited. Content may change prior to final publication. Citation information: DOI 10.1109/ACCESS.2020.3028044, IEEE Access

Date of publication xxxx 00, 0000, date of current version xxxx 00, 0000.

Digital Object Identifier 10.1109/ACCESS.2020.DOI

Vehicle Side-Slip Angle Estimation of Ground Vehicles Based on a Lateral Acceleration Compensation

KWANGHYUN CHO[1], HYUNWOO SON[2], YAFEI WANG[3], (Member, IEEE), KANGHYUN NAM[4], (Member, IEEE), SEIBUM CHOI[5], (Member, IEEE)

[1]Manufacturing Technology Center, Samsung Electronics Co., Ltd., Gyeonggi-do 443-742, South Korea (e-mail: khcho0960@gmail.com)
[2]Plant Intelligent Team, Samsung SDS Co., Ltd., Songpa-gu, Seoul, South Korea (e-mail: hyunwoo.sohn@samsung.com)
[3]School of Mechanical Engineering, Shanghai JiaoTong University, Shanghai 200240, China (e-mail: wyfjlu@sjtu.edu.cn)
[4]School of Mechanical Engineering, Yeungnam University, 280 Daehak-ro, Gyeongsan 712-749, South Korea (e-mail: khnam@yu.ac.kr)
[5]Korea Advanced Institute of Science and Technology, Daejeon 34141, South Korea (e-mail: sbchoi@kaist.ac.kr)

Corresponding author: Kanghyun Nam (e-mail: khnam@yu.ac.kr) and Seibum Choi (e-mail: sbchoi@kaist.ac.kr).

This work was supported by the National Research Foundation of Korea(NRF) grant funded by the Korea government(MSIT) (No. 2019R1F1A1061548) and in part by the Yeugnam University Research Grant 219A380011.

ABSTRACT For vehicle stability control system to function properly under a variety of changing road conditions and driver's inputs, precise estimations of vehicle states are necessarily required. In particular, information on the side-slip angle is critical to vehicle handling and safety control. Since commercial sensors measuring the side-slip angle are not cost effective, estimation methods that use available sensor measurements and vehicle dynamics models are necessarily required. This paper proposes a novel methodology to estimate the side-slip angle which is used as an index of vehicle stability. A side-slip angle observer is designed using the bicycle model and the kinematic model. Here, in order to directly use the lateral accelerometer signal, the lateral acceleration compensation method through the roll angle estimation is proposed. The estimation performance is verified under various road conditions and different driver's inputs using HIL test equipment including commercial vehicle dynamics simulation software CarSim.

INDEX TERMS Lateral acceleration compensation, ground vehicle, observers, roll angle, side-slip angle.

I. INTRODUCTION

As increasing parts of the automobiles rapidly become digitalized, numerous high-performance vehicle stability controllers are being developed [1]. Generally, the vehicle stability control system is a device which secures stability through observing the vehicle states and driver's inputs on the real-time basis. Although a vehicle requires numerous sensors for this purpose, typical vehicles use only the minimum number of the sensors of absolute necessity due to cost issue. This has inspired the development of various observers to estimate the vehicles states of interest, and research projects to extend their performances are ongoing. However, observer design accompanies numerous limitations since it is nearly impossible to account for the strong nonlinear nature of the vehicle characteristics, non-predictability of the road conditions, and irrational intentions of the drivers. For instance, lateral vehicle dynamics control system-that is, in case of ESP-uses the side-slip angle as an index indicating the vehicle stability along with the yaw rate. And here, unlike the yaw rate which is measured through a sensor, the side-slip angle is estimated by an observer. Of course, the side-slip angle can be either directly or indirectly measured using a GPS or an optical sensor. [2] However, the results obtained this way are severely sensitive to the variation of the surroundings and weather. Consequently, the reliability of the measurement is low, and it surely involves additional cost. To solve this issue, numerous research projects have been heading to explore an effective way to indirectly estimate the side-slip angle. [3]–[12], [19]–[24] Due to the extremely nonlinear characteristics of the suspension, the results are bound by limitations for guaranteeing robust performance in various situations. Fukada approached through an estimation method based on the lateral force directly integrated using the acceleration information and the side-slip angle observer that is designed on the basis of the linear tire model. [5] However this approach involves a theoretical problem concerning its

This article has been accepted for publication in a future issue of this journal, but has not been fully edited. Content may change prior to final publication. Citation information: DOI 10.1109/ACCESS.2020.3028044, IEEE Access

stability, and entails limitations regarding the vehicle dynamics since the tire characteristic exhibits severely non-linear region during the maneuvers like J-turn. Farrelly and Wellstead proposed a kinematics model-based linear time-variant observer. [3] This model is certified for the robust performance toward the modeling uncertainty and nonlinear nature, but it neglects the analysis of the accelerometer error and road disturbance including roll and pitch angle that critically affect the observer performance. Kaminaga and Naito proposed the adaptive observer which satisfies Lyapunov stability condition to the tire stiffness variation, and verified its effectiveness even in the strongly nonlinear region, but there existed the condition of persistent excitation to be met. [9] H. Lee proposed a lateral velocity observer based on a simple bicycle model, but it involved an uncertified assumption in the process of obtaining the observer gain for the theoretical analysis, and neglected the effect of the uncertainty related to an accelerometer. [11] H. Kim and D. Pi proposed a side-slip observer using the extended kalman filter, but it used the lateral accelerometer directly and it neglected the road disturbance such as road bank angle. Also, this method has severe computational burden because it uses the extended kalman filter. [23]–[25]

In this paper, to solve the issue of side-slip angle observation, a novel concept is developed based on a modified bicycle model using lateral acceleration information. It is a type of observer that combines the advantages of two conventional models: the bicycle model that is sensitive to vehicle parameters but insensitive to sensor bias due to the absence of a lateral accelerometer, and the kinematic model that includes a lateral acceleration information but does not effective on the vehicle parameters. Using the combination of both models and compensating the lateral accelerometer from the sensor offset such as the gravity component, the robust side-slip angle observer is designed. In addition, a new roll angle estimation methodology is proposed to compensate the drifting issue of a lateral accelerometer which is directly used for the observer. By obtaining the realistic lateral acceleration component which excludes gravitational effect, the issue with the lateral accelerometer-that it is easily disturbed by various road conditions and driver's inputs-is resolved. The performance of the recommended observer is verified through simulations under various conditions using HIL test equipment.

This paper consists of the following. In section II, an analysis and issue of the conventional side-slip angle observer design are addressed, and a new observer with the use of the modified bicycle model is presented. In section III, a compensation method for the roll angle is presented. In section IV, in order to verify the performance of each designed observer, HIL tests in various conditions are carried out. In section V, a summary of the paper is presented to conclude it.

II. SIDE-SLIP ANGLE OBSERVER

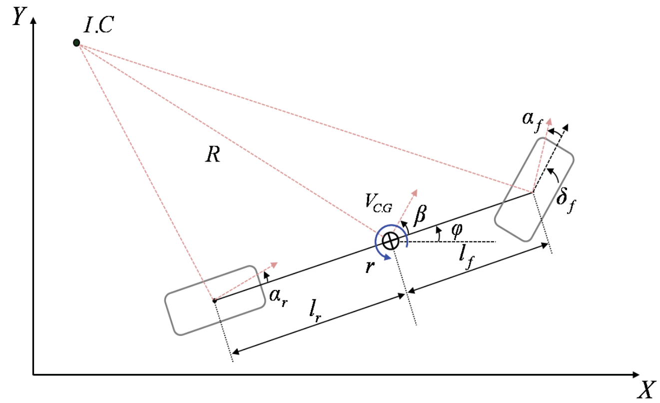

FIGURE 1. Bicycle model for a front steering vehicle

A. BICYCLE MODEL

The lateral motion of a vehicle is typically explained based on the bicycle model. The bicycle model shown in Fig. 1 is a linearized model under the assumptions that the vehicle longitudinal velocity v_x is constant and the tire cornering stiffness, C_f and C_r are symmetric laterally. It is a simple model which requires minimum amount of calculation and relatively efficient in its performance. Although it is very susceptible to the vehicle parameter and the road conditions, it does not directly use the lateral accelerometer in estimating the side-slip angle β but rather use the yaw rate sensor r which is relatively reliable. Therefore the bicycle model owns an advantage for it is well-guarded from the influence of the sensor error. The dynamics model based on the bicycle model is derived from the following force balance and moment balance equations.

$$ma_y = F_{yf} + F_{yr} \tag{1}$$

$$I_z\dot{r} = F_{yf}l_f - F_{yr}l_r \tag{2}$$

where m is vehicle mass, I_z is inertia of moment, l_f and l_r are the distance between front and rear tires and the center of inertia. If the vehicle lateral motion is derived in terms of the lateral acceleration a_y in the inertial frame, and the lateral forces of front and rear, F_{yf} and F_{yr}, are expressed in terms of the tire cornering stiffness and the tire side-slip angles, α_f and α_r, the following equations can be derived. For the sake of simplification, nominal value of the cornering stiffness is fixed at zero tire side-slip angle.

$$a_y = \dot{v}_y + rv_x \tag{3}$$

$$\alpha_f = \beta + r\frac{l_f}{v_x} - \delta_f \tag{4}$$

$$\alpha_r = \beta - r\frac{l_r}{v_x} \tag{5}$$

$$F_{yf} = -2C_f\big|_{\alpha_f=0}\alpha_f \tag{6}$$

This article has been accepted for publication in a future issue of this journal, but has not been fully edited. Content may change prior to final publication. Citation information: DOI 10.1109/ACCESS.2020.3028044, IEEE Access

$$F_{yr} = -2C_r\big|_{\alpha_r=0}\alpha_r \tag{7}$$

where v_y is lateral velocity, and δ_f is steering angle. If the longitudinal velocity of the vehicle is constant, the derivative of the side-slip angle (8) is expressed as (9).

$$\beta \approx \frac{v_y}{v_x} \tag{8}$$

$$\dot{\beta} = \frac{\dot{v}_y}{v_x} \tag{9}$$

Using the above equations, the following state-space equations of the bicycle model are derived.

$$\dot{x} = Ax + Bu, \qquad A \in R^{2\times2}, \quad B \in R^{2\times1} \tag{10}$$

$$y = Cx, \qquad C \in R^{1\times2} \tag{11}$$

where,

$$A = \begin{bmatrix} -\frac{2(C_f+C_r)}{mv_x} & \frac{2(C_r l_r - C_f l_f)}{m{v_x}^2} - 1 \\ \frac{2(C_r l_r - C_f l_f)}{I_z} & -\frac{2(C_f {l_f}^2 + C_r {l_r}^2)}{I_z v_x} \end{bmatrix}, B = \begin{bmatrix} \frac{2C_f}{mv_x} \\ \frac{2C_f l_f}{I_z} \end{bmatrix},$$

$$C = \begin{bmatrix} 0 & 1 \end{bmatrix}, \quad x = \begin{bmatrix} \beta \\ r \end{bmatrix}, \text{and} \quad y = r.$$

B. SIMPLE BICYCLE MODEL-BASED OBSERVER

For the estimation of the side-slip angle, a simple Luenberger observer is designed from (10) and (11). Since it is a linear time-invariant system, the error value is made to approach zero by the negative pole-placement method. This satisfies the asymptotical stability.

$$\dot{\hat{x}} = A\hat{x} + Bu + K_b(y - \hat{y}), \quad K_b \in R^{2\times1} \tag{12}$$

$$\hat{y} = C\hat{x}, \qquad C \in R^{1\times2} \tag{13}$$

If the influence of the model uncertainty and sensor error is neglected, the observer gain value K_b can be obtained through the error dynamics equation. To satisfy the stability of the system, all poles must have negative values. In here, all poles are designed to have the same value of p for simplicity.

$$\dot{\tilde{x}} = (A - K_b C)\tilde{x} \tag{14}$$

$$det(sI - (A - K_b C)) = (s-p)^2, \qquad p < 0 \tag{15}$$

The gain value to meet the desired pole location, p, is calculated as follows from (15).

$$K_{b1} = -\frac{I_z p^2}{2(C_f l_f - C_r l_r)} - \frac{2(C_f l_f - C_r l_r)}{mv_x} + 1 \tag{16}$$

$$K_{b2} = -2\frac{(C_f + C_r) + (C_f {l_f}^2 + C_r {l_r}^2) + p}{I_z m v_x} \tag{17}$$

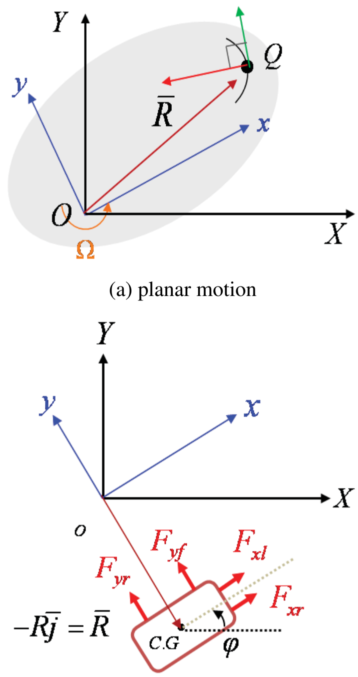

(b) vehicle motion

FIGURE 2. Kinematic model

C. KINEMATIC MODEL

Bicycle model-based observer has the issues of sensitivity to model parametric uncertainty and oversensitivity to road conditions. In contrast, the kinematic model shows an independent nature regarding the vehicle model parameters and road conditions. However, since it uses the longitudinal/lateral accelerometer and the estimated longitudinal velocity, the kinematic model is not robust to the sensor error, and thus requires an appropriate compensation. Fig. 2 describes the kinematic model used for the vehicle motion.

$$\dot{v}_x = r(t)v_y + a_x + w_x \tag{18}$$

$$\dot{v}_y = -r(t)v_x + a_y + w_y \tag{19}$$

$$y = v_x + s_x \tag{20}$$

where w_x and w_y mean unknown uncertainties.

The kinematic model is expressed as a linear time-variant system in terms of the yaw rate $r(t)$. Here, the measurement, y represents a longitudinal vehicle speed which is estimated based on the undriven wheel speeds. Therefore, it includes the pure longitudinal velocity, v_x and the sensor error, s_x which is the uncertainty due to the roll, pitch and others.

D. KINEMATIC MODEL-BASED OBSERVER

For the sideslip angle estimation, a Luenberger observer is designed from (18), (19) and (20) as follows.

$$\dot{\hat{x}} = (A_k(t) - K_k(t)C_k)\hat{x} + B_k t)u + K_k(t)y, \quad K_k \in R^{2\times1} \tag{21}$$

This article has been accepted for publication in a future issue of this journal, but has not been fully edited. Content may change prior to final publication. Citation information: DOI 10.1109/ACCESS.2020.3028044, IEEE Access

$$\dot{\tilde{x}} = (A_k(t) - K_k(t)C_k)\tilde{x} + w - K_k(t)s_x \tag{22}$$

where,

$$A_k(t) = \begin{bmatrix} 0 & r(t) \\ -r(t) & 0 \end{bmatrix}, \quad B_k = \begin{bmatrix} 1 & 0 \\ 0 & 1 \end{bmatrix},$$

$$C_k = \begin{bmatrix} 1 & 0 \end{bmatrix}, \quad x = \begin{bmatrix} v_x \\ v_y \end{bmatrix}, \text{and} \quad u = \begin{bmatrix} a_x \\ a_y \end{bmatrix}.$$

Since this observer $K_k(t) = [K_{k1}(t) \quad K_{k2}]^T$ is a time-variant system, the simple negative pole placement method cannot be used. Instead, a frozen-time pole placement method like what is shown in (23) is taken to calculate the stable observer gain. [13]

$$det(sI-(A(t)-K_k(t)C(t))) = (s+\alpha|r(t)|)^2, \; \alpha > 0 \tag{23}$$

The primary calculated observer gains are as follows.

$$K_{k1}(t) = 2\alpha|r(t)| \tag{24}$$

$$K_{k2}(t) = (\alpha^2 - 1)r(t) \tag{25}$$

From (21) and (22), the gains are observed to vary effectively in the stable region according to the change of the yaw rate. With the observer gain described as (24) and (25), a Lyapunov function V is defined as follows to evaluate the stability of error dynamics.

$$V(\tilde{v}_x, \tilde{v}_y) = \frac{\alpha^2 \tilde{v}_x^2 + \tilde{v}_y^2}{2} > 0, \quad \forall x = [\tilde{v}_x, \tilde{v}_y] \in R^2 \tag{26}$$

$$\begin{aligned} \tfrac{dV(\tilde{v}_x, \tilde{v}_y)}{dt} &= -2\alpha^3|r(t)|\tilde{v}_x^2 + (\alpha^2 w_x - 2\alpha^3|r(t)|s_x)\tilde{v}_x \\ &\quad +(w_y + (1-\alpha^2)r(t)s_x)\tilde{v}_y \end{aligned} \tag{27}$$

Assuming that the acceleration sensor input of the kinematic model is properly compensated and the longitudinal velocity estimated from the undriven wheel speeds is fairly accurate, (27) can be rewritten as follows.

$$\dot{\tilde{v}}_x = -2\alpha|r(t)|\tilde{v}_x + r(t)\tilde{v}_y \tag{28}$$

$$\dot{\tilde{v}}_y = -\alpha^2 r(t)\tilde{v}_x \tag{29}$$

Therefore,

$$\tfrac{dV(t,x)}{dt} = -2\alpha^3|r(t)|\tilde{v}_x^2 \leq 0, \quad \forall x = [\tilde{v}_x, \tilde{v}_y] \in R^2 - [0,0] \tag{30}$$

For (28), (29) and (30), the asymptotical stability can be verified via LaSalle's theorem. The estimated lateral velocity can also be expressed in terms of side-slip angle by (8).

E. MODIFIED BICYCLE MODEL-BASED OBSERVER

The conventional bicycle model uses only the yaw rate as a measurement. This paper proposes a type of bicycle model assuming that a vehicle has a lateral accelerometer additionally mounted. The advantage of the original bicycle model in high mu condition, where it effectively estimates the side-slip angle relatively free from the sensor error, and the advantage of the kinematic model in low mu nonlinear tire dynamics region, where it is insensitive to vehicle parameters, are both combined in this model.

Using (3) and (9) can be expressed to include the side-slip angle term and the yaw rate term as follows.

$$a_y = \dot{v}_y + rv_x \approx v_x(\dot{\beta} + r) \tag{31}$$

When the conventional bicycle model is associated with $\dot{\beta}$ in (10), output (11) and (31), then a new output equation is obtained.

$$a_y = -\frac{2(C_f + C_r)}{m}\beta - \frac{2(C_f l_f - C_r l_r)}{mv_x}r + \frac{2C_f}{m}\delta_f \tag{32}$$

Since the modified bicycle model is a linear time-invariant system, stability of the observer can easily be satisfied via negative pole placement method.

The equation of the designed observer is as follows.

$$\dot{\hat{x}} = A\hat{x} + Bu + K(y - \hat{y}), \qquad K \in R^{2\times 2} \tag{33}$$

$$\hat{y} = C\hat{x} + Du, \qquad C \in R^{2\times 2} \tag{34}$$

where,

$$A = \begin{bmatrix} A_{11} & A_{12} \\ A_{21} & A_{22} \end{bmatrix} = \begin{bmatrix} -\frac{2(C_f+C_r)}{mv_x} & \frac{2(C_r l_r - C_f l_f)}{m{v_x}^2} - 1 \\ \frac{2(C_r l_r - C_f l_f)}{I_z} & -\frac{2(C_f {l_f}^2 + C_r {l_r}^2)}{I_z v_x} \end{bmatrix},$$

$$B = \begin{bmatrix} \frac{2C_f}{mv_x} \\ \frac{2C_f l_f}{I_z} \end{bmatrix}, \quad C = \begin{bmatrix} 0 & 1 \\ -\frac{2(C_f+C_r)}{m} & -\frac{2(C_f l_f - C_r l_r)}{mv_x} \end{bmatrix},$$

$$K = \begin{bmatrix} K_{11} & K_{12} \\ K_{21} & K_{22} \end{bmatrix}, \quad D = \begin{bmatrix} 0 \\ \frac{2C_f}{m} \end{bmatrix}, \hat{x} = \begin{bmatrix} \beta \\ r \end{bmatrix},$$

$$u = \delta_f, \quad y = \begin{bmatrix} r \\ a_y \end{bmatrix}, \quad \hat{y} = \begin{bmatrix} \hat{r} \\ \hat{a}_y \end{bmatrix},$$

where, $\hat{a}_y$ is defined from (32) with β and r replaced by $\hat{\beta}$ and $\hat{r}$.

Here, the error dynamics concerning the side-slip angle is derived using (10), (33) and (34) as follows.

$$\begin{aligned} \dot{\tilde{\beta}} &= A_{11}(1 - K_{12}v_x)\tilde{\beta} + A_{12}(1 - K_{12}v_x)\tilde{r} \\ &\quad -(K_{11} + K_{12}v_x)\tilde{r} \end{aligned} \tag{35}$$

where, $\tilde{\beta}$ and $\tilde{r}$ are equal to β-$\hat{\beta}$ and r - $\hat{r}$.

This article has been accepted for publication in a future issue of this journal, but has not been fully edited. Content may change prior to final publication. Citation information: DOI 10.1109/ACCESS.2020.3028044, IEEE Access

To provide an independent nature about the model uncertainty, setting the observer gain K_{12} as $\frac{1}{v_x}$ makes the equation considerably simpler, and turning (35) into the following

$$\dot{\tilde{\beta}} = -(1 + K_{11})\tilde{r} \tag{36}$$

Other gain values are defined as follows using negative pole placement method.

$$K = \begin{bmatrix} \frac{I_z(l_f C_f - l_r C_r)p^2}{2C_f C_r (l_f + l_r)^2} - 1 & \frac{1}{v_x} \\ -2p & \frac{m(l_f{}^2 C_f + l_r{}^2 C_r)}{I_z(l_f C_f - l_r C_r)} \end{bmatrix} \tag{37}$$

Final design of the observer is defined as follows.

$$\dot{\hat{\beta}} = -\frac{I_z\left(C_f l_f - C_r l_r\right)p^2}{2C_f C_r L^2}\hat{r} + \left(\frac{I_z\left(C_f l_f - C_r l_r\right)p^2}{2C_f C_r L^2} - 1\right)r + \frac{a_y}{v_x} \tag{38}$$

$$\dot{\hat{r}} = -\frac{2C_f C_r L^2}{I_z\left(C_f l_f - C_r l_r\right)}\hat{\beta} + 2p\hat{r} - \frac{2C_f C_r L^2}{I_z\left(C_f l_f - C_r l_r\right)}\delta_f - 2pr + \frac{m\left(C_f l_f{}^2 + C_r l_r{}^2\right)}{I_z\left(C_f l_f - C_r l_r\right)}a_y \tag{39}$$

As it can be seen in (38), lateral acceleration a_y is directly used to estimate the side-slip angle. To use the lateral accelerometer signal for the estimation, the compensation of the gravity component must be done by estimating the roll angle of the vehicle.

III. ROLL ANGLE ESTIMATION FOR COMPENSATING LATERAL ACCELERATION MEASUREMENT

This section discusses the estimation of the roll angle for compensating the lateral accelerometer signal. The roll motion of the vehicle causes the lateral accelerometer to read gravity. This gravity component makes the direct use of the lateral accelerometer very problematic because it causes the sensor offset. Therefore, the exact estimation of the roll angle must be performed to compensate for the lateral accelerometer sensor bias. Many researches have been performed to estimate the roll angle of the vehicle. However, they have the issue of sensing sensitivity due to the nonlinear characteristics or coupling problem with the lateral velocity observer. [5] [14] Recently, the research using GPS has been also in progress. However, application to real vehicles is still in difficulty due to the cost issue as well as the robustness of GPS signal itself. [2] In Tseng's research, the estimation of the overall road bank angle was conducted. [16] [17] [18] Tseng proposed a method which decouples the effect of the road bank and the lateral dynamics in steady state conditions, but its performance is deteriorated during the transient states where the suspension angle is not necessarily zero even on leveled ground like when a sudden step, slalom, or double lane change steering input is fed. This paper proposes a new roll angle estimation method using a roll index which

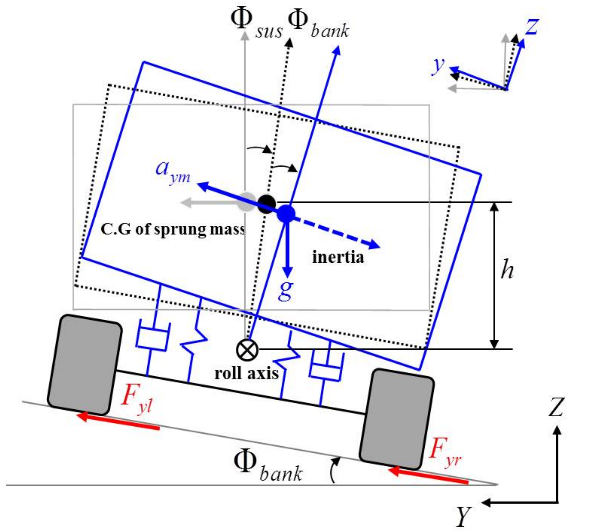

FIGURE 3. Vehicle roll model(ISO 8855 coordinate)

is defined reflexing the vehicle states such as suspension angle and static bank angle through the contemplation of the previous researches. This paper assumes that the pure sensor offset except the gravity component is compensated already using sensor zeroing process. [26] [27]

A. ESTIMATION OF SUSPENSION ROLL ANGLE

The rolling of a vehicle can occur due to the centripetal force caused by the lateral force and road bank angle as described in (40) and also shown in Fig. 3.

$$\Phi_{roll} = \Phi_{sus} + \Phi_{bank} \tag{40}$$

While the vehicle is making a flat surface maneuver, rolling is caused by the suspension system in motion. Suspension model is often considered as equivalent to a spring and damper system. Here, to derive the suspension model, the following assumptions are made.

- roll axis is not varying with the vehicle roll angle.
- roll stiffness and damping coefficient are constants.
- pure heave motion of the vehicle is negligible.
- The center of gravity position and mass of the vehicle are constants.

With these assumptions, a 2nd-order dynamic model of the suspension is derived as follows.

$$I_r\ddot{\Phi}_{sus} = ma_{ym}h - d_{sus}\dot{\Phi}_{sus} - k_{sus}\Phi_{sus} \tag{41}$$

$$I_r = I_{C.G} + mh^2 \tag{42}$$

In this paper, suspension roll angle is estimated via open-loop integration method assuming that a roll rate sensor is absent due to a cost issue. Also at a steady state, (41) can be further simplified as follows.

$$\Phi_{sus} \approx \Phi_{sus-ss} = \frac{hm}{k_{sus}} a_{ym} \tag{43}$$

(43) can be used to compensate for the steady state bias of the lateral acceleration sensor signal due to gravity.

B. ESTIMATION OF STATIC BANK ANGLE

(3) can be expressed as follows using the measured lateral acceleration a_{ym} and the vehicle roll angle Φ_{roll}.

$$a_{ym} + g\sin(\Phi_{roll}) = \dot{v}_y + rv_x \tag{44}$$

Therefore,

$$\Phi_{roll} = \sin^{-1}\left(\frac{\dot{v}_y + rv_x - a_{ym}}{g}\right) \approx \frac{\dot{v}_y + rv_x - a_{ym}}{g} \tag{45}$$

In (44), $\dot{v}_y$ is not the readily available information. When the lateral motion of a vehicle is mild enough to be neglected in presence of the road bank angle, i.e. $\dot{v}_y \approx 0$, (45) is expressed as follows.

$$\Phi_{roll} = \Phi_{ss} = \sin^{-1}\left(\frac{rv_x - a_{ym}}{g}\right) \approx \frac{rv_x - a_{ym}}{g} \tag{46}$$

Here, Φ_{ss} is defined as the static bank angle.

C. ESTIMATION OF DYNAMIC BANK ANGLE USING DFC

The estimation of static bank angle degenerates rapidly in the transient region where the vehicle dynamics controller is usually activated. For this reason, Tseng proposed a method to decouple the lateral dynamics component from the road bank angle based on the static bank angle estimated during the steady state maneuver. [16] When (43) is applied to enhance (10) to banked cases, the following relationship can be derived.

$$\dot{\hat{\beta}} = -\frac{2(C_f + C_r)}{mv_x}\beta - \frac{2(C_f l_f + C_R l_r)}{m{v_x}^2} r + \frac{2C_f}{mv_x}\delta_f + \frac{g}{v_x}\sin(\Phi_{roll}) \tag{47}$$

$$\dot{\hat{r}} = -\frac{2(C_f l_f + C_R l_r)}{I_z}\beta - \frac{2(C_f {l_f}^2 + C_R {l_r}^2)}{I_z v_x} r + \frac{2C_f l_f}{I_z}\delta_f \tag{48}$$

If the transfer functions at a steady state are obtained from (47) and (48), they are described as follows. Here, inputs are Φ_{roll} and δ_f, while outputs are a_y and r. L is the length of the wheel base.

$$H_{\Phi_{roll} \mapsto a_y} = \frac{{v_x}^2 k_u g}{L + k_u {v_x}^2} - g \tag{49}$$

$$H_{\Phi_{roll} \mapsto r} = \frac{v_x k_u g}{L + k_u {v_x}^2} \tag{50}$$

$$H_{\delta_f \mapsto a_y} = \frac{v_x^2}{L + k_u {v_x}^2} \tag{51}$$

$$H_{\delta_f \mapsto r} = \frac{v_x}{L + k_u {v_x}^2} \tag{52}$$

Tseng showed the validity of superpositioning for the following equations with some experimental evidences.

$$a_y = H_{\delta_f \mapsto a_y} \cdot \delta_f + H_{\Phi_{roll} \mapsto a_y} \cdot \Phi_{roll} \tag{53}$$

$$r = H_{\delta_f \mapsto r} \cdot \delta_f + H_{\Phi_{roll} \mapsto r} \cdot \Phi_{roll} \tag{54}$$

Here, the roll angles due to a_y and r are defined as follows.

$$\sin(\hat{\Phi}_{a_y}) = {H_{\Phi_{roll} \mapsto a_y}}^{-1}(a_{ym} - H_{\delta_f \mapsto a_y} \cdot \delta_f) \tag{55}$$

$$\sin(\hat{\Phi}_r) = {H_{\Phi_{roll} \mapsto r}}^{-1}(r - H_{\delta_f \mapsto r} \cdot \delta_f) \tag{56}$$

Tseng defined a dynamic factor (DFC) indicating the magnitude of $\dot{v}_y$ that is directly related to the lateral dynamics component as follows.

$$\begin{aligned} DFC = {} & H_{\Phi_{roll} \mapsto a_y} \cdot (\sin\hat{\Phi}_{a_y} - \sin\hat{\Phi}_{ss}) \\ & + v_x \cdot H_{\Phi_roll \mapsto r} \cdot (\sin\hat{\Phi}_r - \sin\hat{\Phi}_{ss}) \end{aligned} \tag{57}$$

In the next equation, dynamic road bank angle is defined using DFC declared in (57).

$$\sin(\hat{\Phi}_{dyn}) = \sin(\hat{\Phi}_{ss}) \cdot \max[0, 1 - |DFC| - |d\sin\hat{\Phi}_{ss}/dt|] \tag{58}$$

D. ESTIMATION OF ROLL ANGLE USING ROLL INDEX

The approach proposed by Tseng and shown in (58) has a problem of canceling suspension roll angle in the dynamic region where DFC is greater than 1. For this issue, a solution is given by multiplying weighting factors according to the frequency of the suspension roll angle and the road bank angle. [18]

$$\Phi_{roll} = \Phi_{dyn\_freq} + \Phi_{ss\_freq} \tag{59}$$

However, this method has some problem in real-time implementation, for it requires numerous calculations.

This paper defines a roll index λ to indicate vehicle states, concerning the characteristic of the roll angle that consists of the combination of the road bank disturbance and the suspension roll angle caused by steering inputs. Using the roll index which indicates the transient or the steady state region, a new algorithm to estimate the overall roll angle is proposed. The roll index is defined considering the correlation of the static angles defined in (46), (55) and (56). In addition, vehicle states are distinguished by the yaw rate induced by the driver's steering inputs and road bank angle. Finally, the roll index λ is defined as follows.

$$\lambda = f\big(\dot{\hat{\Phi}}_{ss}, \dot{\hat{\Phi}}_{a_y}, \dot{\hat{\Phi}}_r\big) \cdot g\big(\hat{\Phi}_{a_y}, \hat{\Phi}_r\big) \cdot h\big(\delta_f, \dot{\delta}_f, r\big) \cdot k\big(\delta_f, r\big) \tag{60}$$

This article has been accepted for publication in a future issue of this journal, but has not been fully edited. Content may change prior to final publication. Citation information: DOI 10.1109/ACCESS.2020.3028044, IEEE Access

where,

$$f = \begin{cases} 1 \quad if \quad \left| \frac{d}{dt}\left(|\dot{\hat{\Phi}}_{a_y} - \dot{\hat{\Phi}}_{ss}| - |\dot{\hat{\Phi}}_{r} - \dot{\hat{\Phi}}_{ss}|\right) \right| < F_{TH} \\ \quad \text{during} \quad t_{TH1} \\ 0 \quad \text{otherwise} \end{cases}$$

$$g = \begin{cases} 1 \quad if \quad \hat{\Phi}_{a_y} \cdot \hat{\Phi}_{r} < 0 \quad \text{during} \quad t_{TH2} \\ 0 \quad \text{otherwise} \end{cases}$$

$$h = \begin{cases} 1 \quad if \quad |\delta_f| < G_{TH1} \quad \text{and} \quad |\dot{\delta}_f| < G_{TH2} \\ \quad \text{and} \quad |r| < G_{TH3} \quad \text{during} \quad t_{TH3} \\ 0 \quad \text{otherwise} \end{cases}$$

$$k = \begin{cases} 1 \quad if \quad \delta_f \cdot r > K_{TH} \quad \text{during} \quad t_{TH4} \\ 0 \quad \text{otherwise} \end{cases}$$

Here, f is a flag which distinguishes between the steady state and the transient region, based on the difference in the overall shapes of the roll angles calculated from (46), (55) and (56), where F_{TH} is set to 25 deg/s^2 and t_{TH1} 0.4 sec. g is a flag that indicates the presence of the road bank angle using $\hat{\Phi}_{a_y}$ and $\hat{\Phi}_r$, where t_{TH2} is set to 0.4 sec. h is a flag that tells whether the vehicle is running straight on a flat surface or not, using the steering input and yaw rate, where G_{TH1}, G_{TH2} and G_{TH3} are set to 0.5 deg, 0.1 deg/s and 0.3 deg/s respectively. k is a flag which shows that the driver has not applied an urgent steering input in the presence of a road bank angle, where K_{TH} is set to 1500 deg^2/s and t_{TH4} 1.5 sec.

Using the roll index the roll angle is estimated as follows. The proposed estimation method considers both suspension roll rate in the transient state and static bank angle in the steady state.

$$\hat{\Phi}_{roll} = (1-\lambda)\left(\int_{t_1}^{t_2} \dot{\hat{\Phi}}_{sus-ss} dt + \hat{\Phi}^{*}_{ss}\right) + \lambda \cdot \hat{\Phi}_{ss} \quad (61)$$

Here, $\hat{\Phi}^{*}_{ss}$ denotes the static bank angle at the moment when the bank index is switching from 1 to 0. Namely, it is used as the initial condition to integrate the suspension roll rate in the region where the roll index is 0. Also, $\hat{\Phi}_{ss}$ and $\dot{\hat{\Phi}}_{sus-ss}$ are the static bank angle and the derivative of the suspension roll angle.

E. LATERAL ACCELERATION COMPENSATION

The measured lateral acceleration reflects the addition of the practical lateral dynamics component and the gravity component by the influence of the road bank disturbance and the driver's steering input. When it comes to the estimator which uses the lateral acceleration, the performance of the estimation is decreased due to the reading of the gravitational component. In this paper, the measured lateral acceleration is compensated using the estimated roll angle derived in (61) as follows.

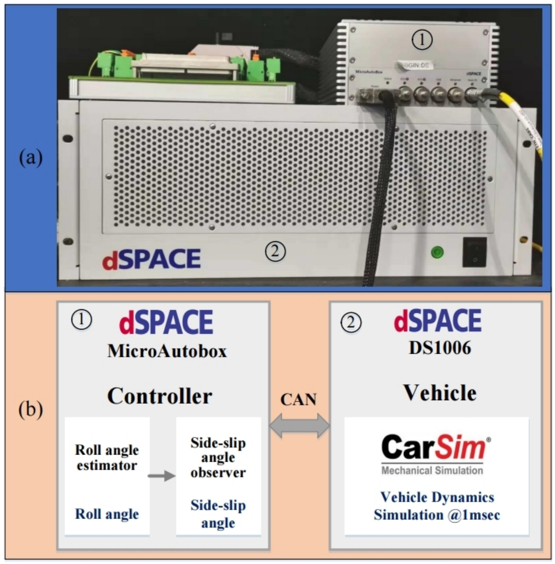

FIGURE 4. Description of Hardware-in-the-loop (HIL) test environment: (a) Real view of HIL test equipment. (b) Components and those functions.

$$a_y = a_{ym} + g \cdot \sin(\hat{\Phi}_{roll}) \quad (62)$$

The compensated lateral acceleration, a_y is used to estimate the side-slip angle of the vehicle at the proposed side-slip angle observer suggested in (38).

IV. PERFORMANCE VERIFICATION

In order to verify the effectiveness of the proposed method, HIL tests were carried out and the testing platform is shown in Fig. 4. The vehicle runs in a DS1006 real-time computer and the designed roll angle estimator and the side-slip angle observer are implemented in a MicroAutobox. The communications between these two equipment are based on the controller area network (CAN). To verify the performance of the proposed method under various road conditions and different driver's inputs, the vehicle is simulated under various conditions using a production simulation software, CarSim, and the vehicle parameters and simulation scenarios are shown in TABLE 1 and TABLE 2.

To verify the performance of roll angle estimation, the actual roll angle(roll actual), that obtained by using Tseng's DFC (roll DFC), and that from the proposed roll angle esti-

TABLE 1. Parameters of the vehicle model

Parameter	Symbol	Value	Unit
Vehicle mass	m	1370	kg
Moment of inertia	I_z	4190	$kg \cdot m^2$
Front Cornering stiffness	C_f	2000	N/deg
Rear Cornering stiffness	C_r	1600	N/deg
Distance from CG to front	l_f	1.110	m
Distance from CG to rear	l_r	1.666	m
C.G. Height above roll axis	h	0.54	m

This article has been accepted for publication in a future issue of this journal, but has not been fully edited. Content may change prior to final publication. Citation information: DOI 10.1109/ACCESS.2020.3028044, IEEE Access

TABLE 2. HIL test scenario

Case.I	· Step steering · high mu(0.85) · 80kph · flat surface
Case.II	· Slalom steering(0.5Hz) · low mu(0.25) · 140kph · flat surface
Case.III	· Straight and bank turn · high mu(0.85) · 80kph · bank angle(0 $\sim$ 25deg)
Case.IV	· Double lane change steering · high mu(0.85 · 80kph · bank angle(0 $\sim$ 16deg)

mator using the roll index are compared. To show the effect of compensating the gravity component out of the measured lateral acceleration, the pure lateral acceleration free from gravity component(actual), measured lateral acceleration(ay w G), and compensated acceleration(ay w/o G) are compared. Furthermore, the performance of the suggested side-slip angle observer using the modified bicycle model(mod-bic) is compared with those of different models presented in section II such as the simple bicycle model(simp-bic) and the kinematic model(kin). The proposed observer shows the effect of the lateral acceleration compensation by comparing the cases of using compensated lateral acceleration(mod-bic) and uncompensated one(mod-bic-w/g).

Fig. 5 and Fig. 6 display the results of dynamic steering maneuvers obtained in the absence of the road bank angle. Fig. 5 shows the case in which a step steer input is fed under the high mu condition like on asphalt, and Fig. 6 considers the case in which a slalom steer input is fed under the low mu condition like on ice. It is observed that the estimation using the roll index which takes the effect of the suspension angle into consideration is more accurate than that in Tseng's work where it only considers the presence of bank angle. Also, in Fig. 5(b) and Fig. 6(b), it is observed that the lateral acceleration not compensated by the estimated roll angle is biased up to $0.5m/s^2$, unlike the cases in which the lateral acceleration is compensated. This biased component leads to the divergence of the estimated side-slip angle as shown in Fig. 5(c) and Fig. 6(c). Concerning the side-slip angle estimation, it is demonstrated that the modified bicycle model gives the most reliable performance regardless of the friction coefficient of the road.

Fig. 7 and Fig. 8 show the results for the case when the road bank disturbance is present. The HIL test result of the vehicle that first runs straight on the flat ground, turns left on the curved road with the road bank angle and then again proceeds onto the straight flat road is given in Fig. 7. Here, it must be addressed that the steering angle is near zero even

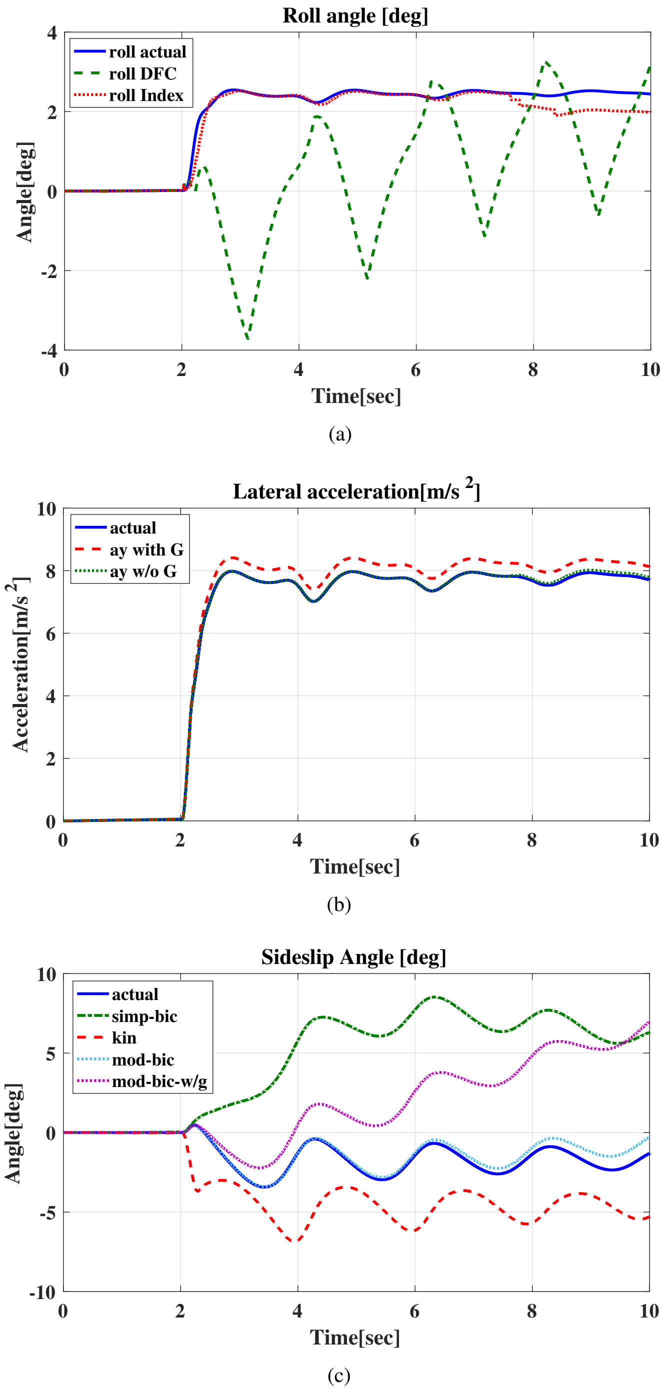

FIGURE 5. HIL test results for Case.I: (a) Roll angle estimation, (b) Lateral acceleration compensation, and (c) Side-slip angle estimation.

when the vehicle is turning left, for it turns naturally due to the severe bank angle. The HIL test result of the vehicle that goes through a double lane change via steering input on the banked road is demonstrated in Fig. 8. In Fig. 7(a), the roll angle is estimated for hardly any steering angle, and the roll angle estimation performance of either method, i.e. using Tseng's DFC or using the roll index, is proven to be effective. It can be seen in Fig. 7(a) that only an insignificant

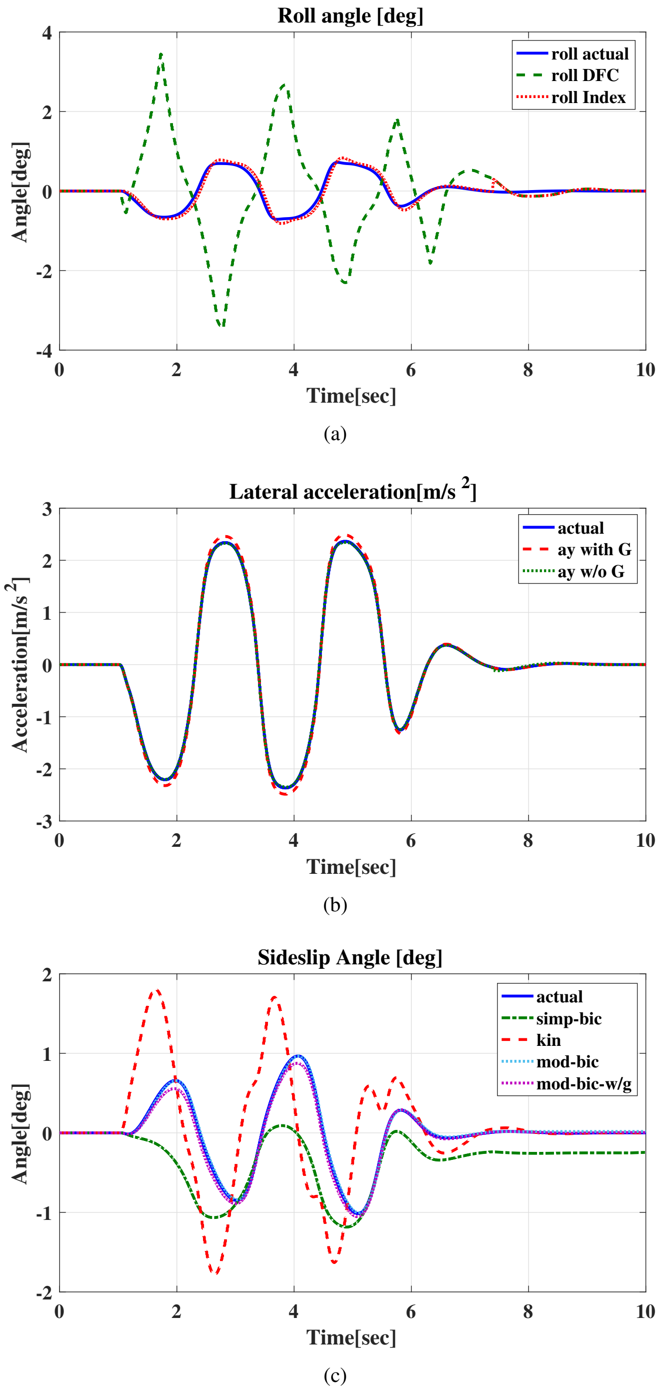

FIGURE 6. HIL test results for Case.II: (a) Roll angle estimation, (b) Lateral acceleration compensation, and (c) Side-slip angle estimation.

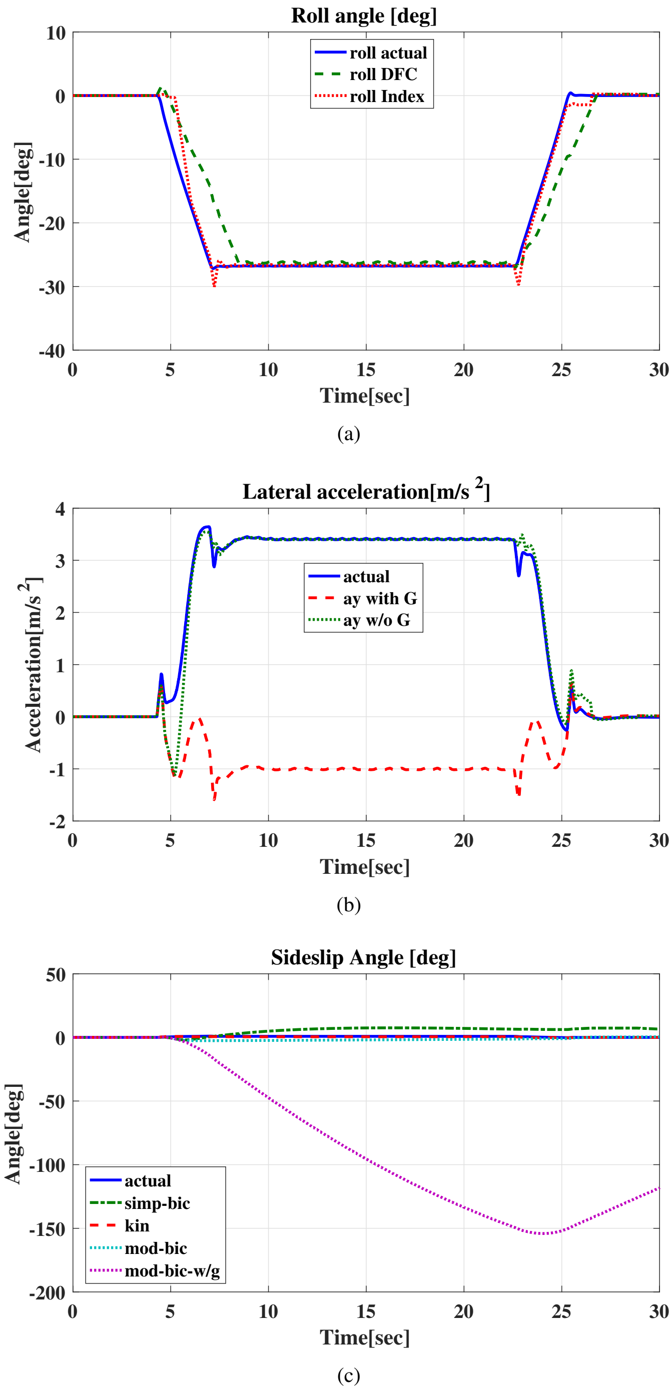

FIGURE 7. HIL test results for Case.III: (a) Roll angle estimation, (b) Lateral acceleration compensation, and (c) Side-slip angle estimation.

amount of delay exists in the estimation result obtained by the roll index model when the bank angle is present (at t=5). This delay is observed to cause some error in compensating for the lateral acceleration, whose result is shown in Fig. 7(b). However, the effectiveness of compensating the lateral acceleration through deleting the gravity component from the road bank is still clearly shown. This improvement is a significant advantage when it comes to estimation of the side-slip angle as well, as shown in Fig. 7(c). Fig. 8(a) is the case in which the suspension roll angle is present. It demonstrates the case in which the suspension roll angle is present due to the steering input on the bank, unlike that in Case III. The proposed method in this paper has some error in roll angle estimation but still shows some improvement compared to the existing methods. Improvement of side-slip estimation in Fig. 8(c) is due to the better lateral acceleration compensation

This article has been accepted for publication in a future issue of this journal, but has not been fully edited. Content may change prior to final publication. Citation information: DOI 10.1109/ACCESS.2020.3028044, IEEE Access

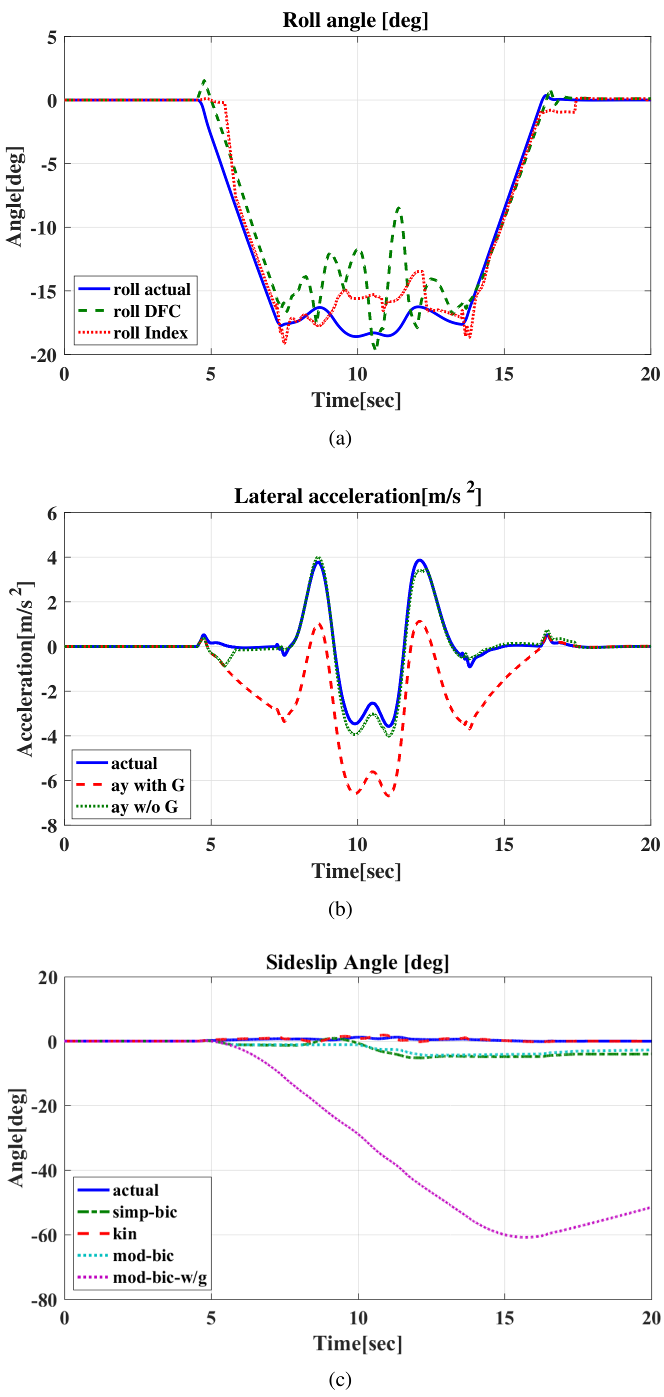

FIGURE 8. HIL test results for Case.IV: (a) Roll angle estimation, (b) Lateral acceleration compensation, and (c) Side-slip angle estimation.

shown in Fig. 8(b).

V. CONCLUSION

This paper presents a side-slip angle observation method using the lateral accelerometer signal directly. To compensate the lateral accelerometer signal bias due to gravity, a vehicle roll angle estimator is designed. The performance of this observer has been verified through HIL tests under various road conditions and steering inputs. As the results show a near-perfect compensation of the lateral acceleration bias improves the performance of the side-slip angle observer significantly. However, the proposed roll angle estimator is found to have a slight amount of error concerning the roll angle estimation due to the switching delay of the roll index. In the future, the model must be supplemented by methods to change the roll index continuously, and to improve the time delay issue due to the binary nature of the roll index. Also, the effect of wide parameter variation such as the longitudinal speed must be considered to expand the application of this study to more dynamic vehicle maneuvers.

APPENDIX. NOMENCLATURE

m	sprung mass.
a_x	actual longitudinal acceleration.
a_y	actual lateral acceleration.
a_{ym}	measured lateral acceleration.
d_{sus}	roll damping coefficient.
k_{sus}	roll stiffness coefficient.
F_{yf}	lateral force of the frontal tire.
F_{yr}	lateral force of the rear tire.
$I_{C.G}$	roll moment of inertia from C.G..
I_r	roll moment of inertia with respect to roll center.
I_z	yaw moment of inertia.
h	height of C.G. from roll axis.
r	yaw rate.
L	wheel base length.
l_f	distance from C.G. to frontal axle.
l_r	distance from C.G. to rear axle.
v_x	true longitudinal velocity.
v_y	true lateral velocity.
α_f	frontal tire side-slip angle.
α_r	rear tire side-slip angle.
C_f	frontal tire cornering stiffness.
C_r	rear tire cornering stiffness.
K	observer gain of the modified bicycle model based observer.
K_b	observer gain of the bicycle model based observer.
K_k	observer gain of the kinematic model based observer.
p	designed pole value.
s_x	longitudinal velocity error.
w_x	longitudinal modeling error of the kinematic model.
w_y	lateral modeling error of the kinematic model.
β	vehicle side-slip angle.
Φ_{roll}	total vehicle roll angle.
Φ_{ss}	static bank angle.
Φ_{sus-ss}	suspension angle at steady state.

REFERENCES

[1] X. Chang, Y. Liu and M. Shen, "Resilient Control Design for Lateral Motion Regulation of Intelligent Vehicle," in *IEEE/ASME Trans. Mechatron.*, vol.

This article has been accepted for publication in a future issue of this journal, but has not been fully edited. Content may change prior to final publication. Citation information: DOI 10.1109/ACCESS.2020.3028044, IEEE Access

24, no. 6, pp. 2488-2497, Dec. 2019.

[2] J. Ryu, E.J. Rossetter, and J.C. Gerdes, "Vehicle sideslip and roll parameter estimation using GPS", *Proc. AVEC*, pp.373-380, 2002.

[3] J. Farrelly, and P. Wellstead, "Estimation of vehicle lateral velocity", *Proc. of the IEEE International Conference on Control Applications*, pp.552-557, 1996.

[4] A.Y. Ungoren, H. Peng, and H.E. Tseng, "A study of lateral speed estimation methods", *International Journal of Vehicle Autonomous Systems*, vol.1, no.1, pp.126-144, 2002.

[5] Y. Fukada, "Slip-angle estimation for vehicle stability control", *Vehicle System Dynamics*, vol.32, no.4, pp.375-388, 1999.

[6] K. Nam, S. Oh, H. Fujimoto, and Y. Hori, "Estimation of sideslip and roll angles of electric vehicles using lateral tire force sensors through RLS and Kalman filter approaches," *IEEE Trans. Ind. Electron.*, vol. 60, no. 3, pp. 988–1000, Mar. 2013.

[7] B. Zhang, H. Du, J. Lam, N. Zhang and W. Li, "A Novel Observer Design for Simultaneous Estimation of Vehicle Steering Angle and Sideslip Angle," *IEEE Trans. Ind. Electron.*, vol. 63, no. 7, pp. 4357–4366, Jul. 2016.

[8] C. Zhang, Q. Chen, and J. Qiu, "Robust H∞ filtering for vehicle sideslip angle estimation with sampled-data measurements", *Transactions of the Institute of Measurement and Control*. vol. 39, no. 7, pp. 1059–1070, Jul. 2017.

[9] M. Kaminaga and G. Naito, "Vehicle body slip angle estimation using an adaptive observer", *Proc. Of AVEC*, vol.98, 1998.

[10] B. Kwak, Y. Park, and D. Kim, "Design of observer for vehicle stability control system", *FISITA World Automotive Congress*, 2000.

[11] H. Lee, "Reliability indexed sensor fusion and its application to vehicle velocity estimation", *Journal of dynamic systems, measurement, and control*, vol.128, no.2, pp.236-243, 2006.

[12] L. Imsland, et al., "Vehicle velocity estimation using nonlinear observers", *Automatica*, vol.42, no.12, pp.2091-2103, 2006.

[13] VC. LeFevre, "The design and implementation of a time-varying observer and an EMA controller for linear systems", *Proc. Southeastern Symposium on SYSTEM THEORY*, pp.297-301, 1997.

[14] J. Hahn, et al., "Road bank angle estimation using disturbance observer", *Proc. Of AVEC 6th international Symposium*, 2002.

[15] J. Ryu, and J.C. Gerdes, "Estimation of vehicle roll and road bank angle", *Proc. American Control Conference*, pp.2110-2115, 2004.

[16] H.E. Tseng, "Dynamic estimation of road bank angle", *Vehicle System Dynamics*, vol.36, no.4-5, pp.307-328, 2001.

[17] L. Xu, and H.E. Tseng, "Robust model-based fault detection for a roll stability control system", *IEEE Trans. on Control Systems Technology*, vol.15, no.3, pp.519, 2007.

[18] H.E. Tseng, and L. Xu, "Robust model-based fault detection for roll rate sensor", *Proc. of the 42nd IEEE Conference on Decision and Control*, vol.2, pp.1968-1973, Dec, 2003.

[19] F. Cheli, et al., "A methodology for vehicle sideslip angle identification:comparision with experimetal data", *Vehicle System Dynamics*, vol.45, no.6, pp.549-563, June, 2007.

[20] S. You, J. Hahn and H. Lee, "New adaptive approaches to real-time estimatio fo vehicle sideslip angle", *Control Engineering Practice*, vol.17, pp.1367-1379, 2009.

[21] G. Baffet, A. Charara, and D. Lechner, "Estimation of vehicle sideslip, tire force and wheel cornering stiffness", *Control Engineering Practice*, vol.17, pp.1255-1264, 2009.

[22] J. Stephant, A. Charara, and D. Meizel, "Evaluation of a sliding mode observer for vehicle sideslip angle", *Control Engineering Practice*, vol.15, pp.803-812 2007.

[23] H. Kim, and J. Ryu, "Sideslip angle estimation considering short-duration longitudinal velocity variation", *International Journal of Automotive Technology*, vol.12, no.4, pp.545-553 2011.

[24] D. Pi, N. Chen, J. Wang and B. Zhang, "Design and evaluation of sideslip angle observer for vehicle stability control", *International Journal of Automotive Technology*, vol.12, no.3, pp.391-399 2011.

[25] M. Doumiati, A. C. Victorino, A. Charara, and D. Lechner, "Onboard real–time estimation of vehicle lateral tire–road forces and sideslip angle," *IEEE/ASME Trans. Mechatron.*, vol. 16, no. 4, pp. 601–614, Aug. 2011.

[26] S.B. Choi, "Practical vehicle rollover avoidance control using energy method", *Vehicle System Dynamics*, vol.46, no.4, pp.323-337 2008.

[27] S.B. Choi, "Antilock brake system with a continuous wheel slip control to maximize the braking performance and the ride quality", *IEEE Transaction on Control Systems Technology*, vol.16, no.5, pp.996-1003 2008.

KWANGHYUN CHO (S'11–M'16) received the B.S. degree in electrical engineering and computer science from Kyungpook National University, Daegu, Korea, in 2008, and the M.S., and Ph.D. degrees in mechanical engineering from Korea Advanced Institute of Science and Technology (KAIST), Daejeon, Korea, in 2010 and 2014, respectively. He is currently a Senior Engineer at Mechatronics R&D Center, Samsung Electronics Co., Ltd., Hwaseong-si, Gyeonggi-do, Korea. His research interests include precision motion control based on linear motors.

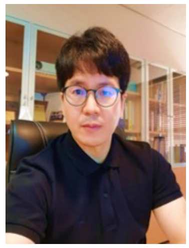

KANGHYUN NAM (S'10–M'12) received the B.S.degree in mechanical engineering from Kyungpook National University, Daegu, Korea, in 2007, the M.S.degree in mechanical engineering from Korea Advanced Institute of Science and Technology, Daejeon, Korea, in 2009, and the Ph.D.degree in electrical engineering from The University of Tokyo, Tokyo, Japan, 2012.

From 2012 to 2015, he was a Senior Engineer with Samsung Electronics Co., Ltd., Gyeonggi-do, Korea. Since 2015, he has been an Assistant Professor with the School of Mechanical Engineering, Yeungnam University, Gyeongbuk, Korea. His research interests include motion control, vehicle dynamics and control, electric vehicles.

Dr. Nam is a member of the Korean Society of Automotive Engineers. He received the 2013 Best Paper Award from the IEEE TRANSACTION ON INDUSTRIAL ELECTRONICS in 2014.

HYUNWOO SON received the B.S. degree in electrical engineering and computer science from Kyungpook National University, Daegu, Korea, in 2007, and the M.S. degrees in mechanical engineering from Korea Advanced Institute of Science and Technology (KAIST), Daejeon, Korea, in 2009. Until 2019, He was Senior Researcher at Electrical Engineering R&D Center, Doosan Heavy Industries & Construction Co., Ltd where he was involved in the development of advanced turbine control system. He is currently a Senior Engineer at Plant Intelligent Team, Samsung SDS Co., Ltd., Songpa-gu, Seoul, Korea. His research interests include advanced utility control and data-driven optimization of manufacturing process.

YAFEI WANG (S'12–M'14) received the B.S. degree in internal combustion engine from Jilin University, Changchun, China, in 2005, the M.S. degree in vehicle engineering from Shanghai Jiao Tong University, Shanghai, China, in 2008, and the Ph.D. degree in electrical engineering from the University of Tokyo, Tokyo, Japan, in 2013.

From 2008 to 2010, he was with automotive industry for nearly two years. From 2013 to 2016, he was a Postdoctoral Researcher with the University of Tokyo. He is currently a Lecturer with the School of Mechanical Engineering, Shanghai Jiao Tong University, Shanghai, China. He is interested in state estimation and control for connected and automated vehicles.

SEIBUM CHOI (M'9) received the B.S. degree in mechanical engineering from Seoul National University, Seoul, South Korea, in 1985, the M.S. degree in mechanical engineering from the Korea Advanced Institute of Science and Technology (KAIST), Daejeon, South Korea, in 1987, and the Ph.D.degree in control from the University of California, Berkeley, CA, USA, in 1993.

From 1993 to 1997, he was involved in the development of automated vehicle control systems at the Institute of Transportation Studies, University of California. In 2006, he was with TRW, Warren, MI, USA, where he was involved in the development of advanced vehicle control systems. Since 2006, he has been with the faculty of the Department of Mechanical Engineering, KAIST. His current research interests include fuel-saving technologies, vehicle dynamics and control, and active safety systems.